Physics and Imaging in Radiation Oncology 19 (2021) 85–89

Contents lists available at ScienceDirect

Physics and Imaging in Radiation Oncology

journal homepage: www.sciencedirect.com/journal/physics-and-imaging-in-radiation-oncology

The impact of image acquisition time on registration, delineation and image quality for magnetic resonance guided radiotherapy of prostate cancer patients

M.E. Nowee [a], V.W.J. van Pelt [a], I. Walraven [a], R. Simões [a], C.P. Liskamp [a], D.M.J. Lambregts [b], S. Heijmink [b], E. Schaake [a], U.A. van der Heide [a], T.M. Janssen [a,*]

[a] Department of Radiation Oncology, The Netherlands Cancer Institute, Amsterdam, The Netherlands
[b] Department of Radiology, The Netherlands Cancer Institute, Amsterdam, The Netherlands

ARTICLE INFO

Keywords:
Image-Guided radiotherapy
Magnetic Resonance Imaging
Target delineation
Image registration
Image quality
Prostate carcinoma

ABSTRACT

Background and Purpose: Magnetic resonance (MR) guided radiotherapy utilizes MR images for (online) plan adaptation and image guidance. The aim of this study was to investigate the impact of variation in MR acquisition time and scan resolution on image quality, interobserver variation in contouring and interobserver variation in registration.

Materials and Methods: Nine patients with prostate cancer were included. Four T2-weighted 3D turbo spin echo (T2w 3D TSE) sequences were acquired with different acquisition times and resolutions. Two radiologists assessed image quality, conspicuity of the capsule, peripheral zone and central gland architecture and motion artefacts on a 5 point scale. Images were delineated by two radiation oncologists and interobserver variation was assessed by the 95% Hausdorff distance. Seven observers registered the MR images on the planning CT. Registrations were compared on systematic offset and interobserver variation.

Results: Acquisition times ranged between 1.3 and 6.3 min. Overall image quality and capsule definition were significantly worse for the MR sequence with an acquisition time of 1.3 min compared to the other sequences. Median 95% Hausdorff distance showed no significant differences in interobserver variation of contouring. Systematic offset and interobserver variation in registration were small (<1 mm) and of no clinical significance.

Conclusions: Our results can be used to effectively shorten overall fraction time for online adaptive MR guided radiotherapy by optimising the imaging sequence used for registration. From the sequences studied, a sequence of 3.1 min with anisotropic voxels of 1.2 × 1.2 × 2.4 mm^3 provided the shortest acquisition time without compromising image quality.

1. Introduction

With the advance of magnetic resonance (MR) guided radiotherapy, a new paradigm in radiation oncology has emerged allowing daily adaptive radiotherapy [1,2]. By acquiring MR images just prior to treatment, high precision image guidance is feasible [3]. The pre-beam MR images are registered to the reference planning image (computed tomography (CT) or MR). Next, either this registration is directly translated to a shifted plan, or the target and organs at risk are re-contoured on the daily MR and a new plan is made on the daily anatomy [4].

However, this also comes at a cost. Typical time slots using MR guidance are substantially longer compared to conventional linear accelerators [4,5]. This potentially increases intrafraction motion [6] and drives up the cost of the treatment [7]. Therefore, it is relevant to evaluate strategies to shorten the treatment slots, with one possible approach being to optimize the MR acquisition time [8].

In MR guided radiotherapy, the MR images can have a threefold use: registration, delineation and interpretation. Shortening the MR acquisition time, without changing the acquisition volume or the pulse sequence, can be done by changing the image resolution. This however naturally influences image quality, which could hamper registration, delineation and interpretation. Image quality can be studied based e.g. on signal-to-noise ratio, or the modulation transfer function, determined

* Corresponding author at: The Netherlands Cancer Institute, Plesmanlaan 121, 1066 CX Amsterdam, The Netherlands.
E-mail address: t.janssen@nki.nl (T.M. Janssen).

https://doi.org/10.1016/j.phro.2021.07.002
Received 15 April 2021; Received in revised form 3 June 2021; Accepted 1 July 2021

on a phantom. However, from a more pragmatic point of view, the quality of an acquisition is determined by the extent to which the image serves the above-mentioned purposes. We hypothesize that, up to a certain threshold, image quality deterioration only mildly influences the suitability of the acquisition for image guidance, allowing for an optimization between efficiency and quality.

The aim of this study is to develop a method to identify the most optimal sequence for use in MR guided radiotherapy, balancing acquisition time and quality to reduce treatment time for prostate cancer patients [9]. Therefore we investigate image quality, interobserver variation in contouring and interobserver variation in registration for a set of MR sequences with different acquisition times.

2. Materials and Methods

2.1. MRI acquisition

The UMBRELLA 1 (N16UMB, NL 60113.031.16)) study was designed to develop and test MR imaging for MR guided radiotherapy in small cohorts of patients with varying cancer types including prostate cancer. The study was approved by the hospital ethics committee. After informed consent, nine patients with prostate cancer were enrolled in the UMBRELLA 1 study and scanned on the Unity integrated MR scanner/linear accelerator (MR-linac) (Elekta AB, Stockholm, Sweden). The Unity is equipped with a modified Philips Ingenia 1.5 T MRI system (Philips Healthcare, Best, The Netherlands) with a split gradient system and an 8-channel coil system, with 4 channels embedded in the patient couch and 4 channels anteriorly positioned over the patient [10].

For each patient four in-house developed axial T2-weighted 3D turbo spin echo (T2w 3D TSE) MR sequences were acquired. The sequences have been optimized on healthy volunteers before start of the study. The 4 sequences differ in voxel size and acquisition time, a 1.2 mm isotropic voxel with a scan time of 6.3 min, a $1.2 \times 1.2 \times 2.4$ mm^3 voxel and 1.7 mm isotropic voxel both with a scan time of 3.1 and 3.2 min respectively and a 1.8 mm isotropic voxel with a scan time of 1.3 min. In total 36 MRI acquisitions were acquired Detailed scan parameters of each sequence are shown in Table 1.

The four sequences were acquired in the same order for every patient, during their third treatment session. The third session was chosen, in order for the patient to be less anxious during treatment and scan acquisition.

2.2. Image quality

Image quality was independently assessed by two expert radiologists (7 and 14 years of dedicated experience in prostate MRI). Images were scored on five quality criteria, that were each assessed using a five point Likert scale (1: poor; 2: moderate; 3: satisfactory; 4: good; 5: excellent) [11]. The used criteria were: 1. Anatomical distinction between peripheral zone and central gland (both transitional and central zone); 2. conspicuity of the capsule; 3. conspicuity of central gland architecture; 4. motion artefacts and 5. overall image quality. Criterion 5 takes e.g. overall signal/noise, artefacts and resolution of the images into account. The observers were blinded for patient number and sequence and the images were presented in a random order. Per image we use the the average score of both observers for analysis. Acquisitions are compared based on the median scores.

Table 1
Scan parameters. All scans are T2 3D turbo spin echo (TSE) sequences in axial orientation, using time to recovery = 1300 ms, flip angle = 90°, turbo factor = 110, sense factor = 3.5 and refocusing control angle = 80°, 100°, 120°. TE = time to echo, FOV = field of view, NSA = number of averages.

	Voxel size (mm^3)	Reconstruction voxel (mm^3)	Time (mins)	TE (ms)	FOV (mm^3)	NSA
A	1.2 × 1.2 × 1.2	0.57 × 0.57 × 1.2	6.3	129	400 × 448 × 249	2
B	1.2 × 1.2 × 2.4	0.57 × 0.57 × 2.4	3.1	128	400 × 448 × 249	2
C	1.7 × 1.7 × 1.7	0.77 × 0.77 × 1.7	3.2	116	400 × 446 × 249	2
D	1.8 × 1.8 × 1.8	0.51 × 0.51 × 1.8	1.3	117	400 × 448 × 250	1

2.3. Contouring

The prostate was independently contoured according to institutional guidelines on all 36 MR images by two dedicated radiation oncologists (both 1 year of dedicated experience in prostate radiotherapy). Delineations were analyzed on:

(a) a systematic difference between the scan protocols by considering the average volumes of the contours;
(b) interobserver variation as quantified by the 95% Hausdorff distance.

2.4. Registration

Seven experienced radiotherapy technologists (RTTs) registered each MR image rigidly (translations only) to the corresponding planning CT in Monaco 5.4 (Elekta AB, Stockholm, Sweden). Registrations were compared based on:

a) a systematic offset: per patient we determined the mean registration vector over all acquisitions and observers. Next, per acquisition, we determined the mean deviation of all observers from this mean registration vector. We used the median (over all patients) magnitude of this vector as our quantitative measure of a systematic offset per acquisition;
b) interobserver variation: per acquisition and per patient we determined the standard deviation of the seven registration in all three dimensions. We used the median (over all patients) magnitude of this vector as our quantitative measure of a interobserver variation.

2.5. Statistical analysis

Statistical differences between scan protocols were tested using Friedman test with Wilcoxon post-hoc testing using $\alpha = 0.05$.

3. Results

3.1. Image quality

A sample image of each acquisition is shown in Fig. 1. A significant difference between sequences was found in the distinction between the peripheral zone and the central gland ($p = 0.03$). Post-hoc testing showed a significant difference between sequence B and C ($p < 0.01$) and B and D ($p = 0.01$), although median score was 2 in all cases (see Table 2). A significant difference was also found in the conspicuity of the capsule ($p < 0.01$). Post-hoc testing showed sequence D to be (borderline) significantly worse compared to the other sequences (A vs D: $p = 0.04$; B vs D: $p < 0.01$; C vs D: $p = 0.05$). Median score was 3 for D versus 3–4 for the other sequences (see Table 2). Moreover, a significant difference was found in overall image quality ($p < 0.01$). Post-hoc testing showed sequence D to be significantly worse compared to the other sequences (A vs D: $p < 0.01$; B vs D: $p < 0.01$; C vs D: $p < 0.01$). Median score was 2 for D versus 3 for the other sequences (see Table 2). Conspicuity of the central gland architecture and motion artefacts did not significantly differ between sequences ($p > 0.10$ in both cases).

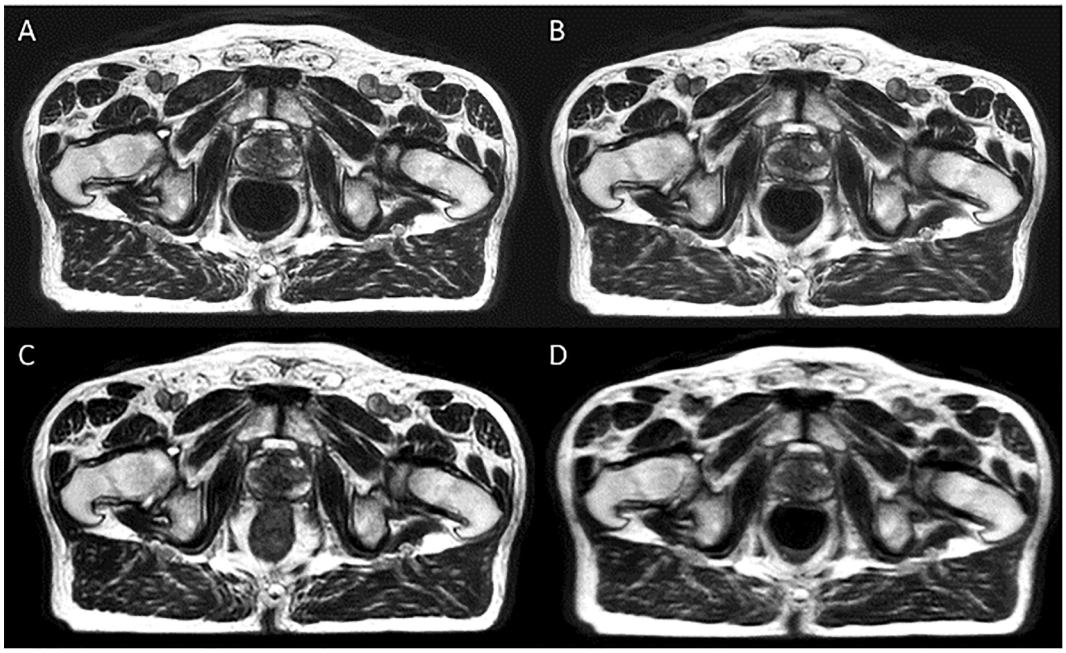

Fig. 1. A sample image of the same patient scanned with the four different scan protocols. A: 1.2 × 1.2 × 1.2 mm^3/6.3 min; B: 1.2 × 1.2 × 2.4 mm^3/3.1 min; C: 1.7 × 1.7 × 1.7 mm^3/3.2 min; D: 1.8 × 1.8 × 1.8 mm^3/1.3 min.

Table 2
Qualitative assessment of image quality. PZ vs PF: peripheral zone vs prostate gland; CG arch.: conspicuity of central gland architecture; Capsule: capsule conspicuity; Motion: motion artefacts and overall: overall image quality. Scores indicate: 1: poor; 2: moderate; 3 Satisfactory; 4: good and 5 excellent. M = median; IQR = inter quartile range. See Table 1 for detailed scan parameters.

	PZ vs PG		CG arch		Capsule		Motion		Overall	
	Median	IQR	Median	IQR	Median	IQR	Median	IQR	Median	IQR
A	2	1.8	2	1	3	1	5	1	3	0.8
B	2	2	2.5	1.8	4	1	5	1	3	1.5
C	2	1	2	2	3.5	2	5	0	3	1
D	2	1	2	1	3	1.8	4	1	2	1

3.2. Contouring variation

The average delineated prostate volume ranged from 47.2 cm^3 (sequence C) to 49.4 cm^3 (sequence B) (see Table 3). No significant difference was found between the sequences in the volumes of the delineations ($p > 0.10$). Contouring interobserver variation ranged from 4.3 mm (sequence A) to 5.1 mm (sequence C) (see Table 3). No significant difference was found in inter-observer variation for the different sequences ($p > 0.10$).

3.3. Registration

Systematic offset of the different scans with respect to the mean of all scans was small, ranging from an average of 0.08 mm (sequences B and C) to 0.1 mm (sequence A) (see Table 3). The differences between sequences was not significant ($p = 0.09$).

Interobserver variation between the registration vectors was small, with a median standard deviation ranging from 0.05 mm (sequences B, C, D) to 0.08 mm for sequence A (see Table 3). A significant difference was found ($p = 0.03$) between sequences. Post-hoc testing showed a statistically significant difference between sequences A and C ($p = 0.03$) and A and D ($p = 0.02$), with in both cases sequence A having the larger interobserver variation.

3.4. Optimal trade-off

Based on the results above, different scan protocols had no relevant influence on contouring and registration accuracy, while in terms of image quality scan B was (slightly) superior compared to the other scans and significantly shorter compared to the high resolution scan A. Therefore we conclude that from the protocols considered scan B is the optimal choice for image guidance, in the sense that it has the shortest

Table 3
Average results on contouring and registration. Std = standard deviation. See Table 1 for detailed scan parameters.

	Contouring				Registration	
	Average volume (cm^3)	Std volume (cm^3)	Median 95% Hausdorff (mm)	25–75 percentiles 95% Hausdorff (mm)	Systematic offset (mm)	Inter-observer variation (mm)
A	48.4	15.8	4.3	3.7–5.6	0.10	0.08
B	49.4	14.5	4.5	2.9–4.8	0.08	0.05
C	47.2	13.2	5.1	3.9–5.7	0.08	0.05
D	47.3	14.6	4.9	3.8–7.9	0.09	0.05

acquisition time, without compromising image quality.

4. Discussion

In this study, we investigated image quality, interobserver variation in contouring and interobserver variation in registration for a set of MR sequences from the Unity MR-linac. While MR acquisitions can be optimized on many different parameters, for interpretability we choose only to vary image resolution and acquisition time. Our method allowed us to select optimal sequences for their intended use.

As far as assessment of the image quality on a 5 point scale is concerned, the lowest resolution scan (D) was significantly worse than the other scans when evaluated on capsule conspicuity and overall image quality. Sequence B was significantly better in terms of the distinction of the peripheral zone versus the central gland. The median quality score of sequences A, B and C was 3, which is only slightly lower compared to the quality score previously reported by Nyholm et al. [11], which reports an average diagnostic image quality for prostate patients of 3.2 using the same five point scale. However, the scores for peripheral zone and central gland conspicuity, are in the range of poor-moderate. Reasons contributing to this are the fact that scans were made on 1.5 T, compared to 3 T and in this work we use T2w 3D TSE sequences instead of diagnostic 2D sequences. Finally, the subjective nature of such a score, complicates a detailed comparison.

Image quality and lesion assessment for prostate cancer on the Unity 1.5 T MR has also been studied before [12,13]. Almansour et al. [13] use a T2w acquisition using $1.5 \times 1.5 \times 2\ mm^3$ voxels and a scan time of just under 2 min. Using a similar qualitative assessment, it was found in agreement with our results, that image quality on the Unity is good and comparable to a diagnostic 3 T scanner, a finding also confirmed by Ullrich et al. [12]. Differences were found in the image quality of diffusion weighted imaging, lesion conspicuity and diagnostic confidence, which is in line with our results where we also saw central gland conspicuity slightly less compared to literature. Also, in line with our results, inter-user variation in quantitative asssements (e.g. volume) was found to be very small. For interobserver contouring variation, no significant difference was found between scan protocols. The interobserver variation we found (median 95% Hausdorff of 4.3–5.1 mm) appears similar to those in [14], where a maximum interobserver variation was found of 4.6 mm for MR based prostate delineation. Pogson et al [15] showed that interobserver variation in contouring increases with decreasing resolution, which is not what we found, however this study was CT based and considered delineation of inserts in a phantom, where no additional uncertainties are present. Since there was also no significant difference in volume between the different sequences, we conclude that all scans are in principle suitable for delineation of the prostate. Registration uncertainty did show systematic differences, however variation of registration in all cases is can be considered small at <0.8 mm for example in contrast with Morrow et al. [16] which showed a reduction of interobserver variation in CT based image guided radiotherapy from 3.2 mm to 1.1 mm registration variation, when comparing MV cone-beam CT with superior kV fan-beam CT. It is interesting to note that the scan protocol with the highest resolution (A; $(1.2\ mm)^3$) actually results in the largest interobserver variation. Apparently, the improved resolution results in different users making slightly different choices. Even for this scan protocol, the variation found is smaller compared to the results presented in [16], where the interobserver variation of prostate match using CBCT is reported to be 2.5 mm. We therefore conclude that for all scan protocols, registration accuracy is sufficient for image guidance, with no clinically relevant differences.

Our results demonstrate that while some sequences may be less suitable for diagnostic purposes such as staging (as reflected in the suboptimal scores on peripheral zone and central gland conspicuity), they are acceptable for target contouring or image registration for treatment guidance. While the specific results of this study are limited to the four sequences evaluated, our methodology can be applied more generally to optimize sequences for the purpose of MR-guided radiotherapy.

Scan protocol time is of course not the only factor influencing overall treatment time. The time required for matching, re-planning, and dose delivery is substantial as well. In particular, for the results presented in this study we should realize that scan resolution might also influence data transfer times and the time required for matching and/or recontouring. Indeed, while there are no significant quantitative differences, the RTTs performing the matching anecdotally indicated that they found it harder to judge the match of the lowest quality scan (D; $(1.8\ mm)^3$), and therefore actually spent more time on the matching procedure and felt less confident with the result. Based on the results of this study we clinically changed our scan protocol from protocol A to protocol B. This way our results have been used to effectively improve overall fraction time for adaptive treatment on the MR-linac by optimising the imaging sequence used for MR guided radiotherapy.

Declaration of competing interest

The authors declare the following financial interests/personal relationships which may be considered as potential competing interests: NKI-AvL is part of the Elekta MR-linac Consortium and we acknowledge financial and technical support from Elekta AB (Stockholm, Sweden) under a research agreement.

References

[1] Acharya S, Fischer-Valuck BW, Kashani R, Parikh P, Yang D, Zhao T, et al. Online magnetic resonance image guided adaptive radiation therapy: first clinical applications. Int J Radiat Oncol Biol Phys 2016;94:394–403. https://doi.org/10.1016/j.ijrobp.2015.10.015.

[2] Raaymakers BW, Jürgenliemk-Schulz IM, Bol GH, Glitzner M, Kotte ANTJ, van Asselen B, et al. First patients treated with a 1.5 T MRI-Linac: Clinical proof of concept of a high-precision, high-field MRI guided radiotherapy treatment. Phys Med Biol 2017;62:L41–50. https://doi.org/10.1088/1361-6560/aa9517.

[3] Raaymakers BW, Lagendijk JJW, Overweg J, Kok JGM, Raaijmakers AJE, Kerkhof EM, et al. Integrating a 1.5 T MRI scanner with a 6 MV accelerator: Proof of concept. Phys Med Biol 2009;54:N229–37. https://doi.org/10.1088/0031-9155/54/12/N01.

[4] Winkel D, Bol GH, Kroon PS, van Asselen B, Hackett SS, Werensteijn-Honingh AM, et al. Adaptive radiotherapy: The Elekta Unity MR-linac concept. Clin Transl Radiat Oncol 2019;18:54–9. https://doi.org/10.1016/j.ctro.2019.04.001.

[5] Corradini S, Alongi F, Andratschke N, Belka C, Boldrini L, Cellini F, et al. MR-guidance in clinical reality: Current treatment challenges and future perspectives. Radiat Oncol 2019;14. https://doi.org/10.1186/s13014-019-1308-y.

[6] Hoogeman MS, Nuyttens JJ, Levendag PC, Heijmen BJM. Time dependence of intrafraction patient motion assessed by repeat stereoscopic imaging. Int J Radiat Oncol Biol Phys 2008;70:609–18. https://doi.org/10.1016/j.ijrobp.2007.08.066.

[7] Van Dyk J, Zubizarreta E, Lievens Y. Cost evaluation to optimise radiation therapy implementation in different income settings: A time-driven activity-based analysis. Radiother Oncol 2017;125:178–85. https://doi.org/10.1016/j.radonc.2017.08.021.

[8] Kurz C, Buizza G, Landry G, Kamp F, Rabe M, Paganelli C, et al. Medical physics challenges in clinical MR-guided radiotherapy. Radiat Oncol 2020;15. https://doi.org/10.1186/s13014-020-01524-4.

[9] Hehakaya C, Van der Voort van Zyp JR, Lagendijk JJW, Grobbee DE, Verkooijen HM, Moors EHM. Problems and promises of introducing the magnetic resonance imaging linear accelerator into routine care: the case of prostate cancer. Front Oncol 2020;10. https://doi.org/10.3389/fonc.2020.01741.

[10] Tijssen RHN, Philippens MEP, Paulson ES, Glitzner M, Chugh B, Wetscherek A, et al. MRI commissioning of 1.5T MR-linac systems – a multi-institutional study. Radiother Oncol 2019;132:114–20. https://doi.org/10.1016/j.radonc.2018.12.011.

[11] Heijmink SWTPJ, Fütterer JJ, Hambrock T, Takahashi S, Scheenen TWJ, Huisman HJ, et al. Prostate cancer: Body array versus endorectal coil MR imaging at 3T - Comparison of image quality, localization, and staging performance. Radiology 2007;244:184–95. https://doi.org/10.1148/radiol.2441060425.

[12] Ullrich T, Quentin M, Oelers C, Dietzel F, Sawicki LM, Arsov C, et al. Magnetic resonance imaging of the prostate at 1.5 versus 3.0 T: A prospective comparison study of image quality. Eur J Radiol 2017;90:192–7. https://doi.org/10.1016/j.ejrad.2017.02.044.

[13] Almansour H, Afat S, Fritz V, Schick F, Nachbar M, Thorwarth D, et al. Prospective image quality and lesion assessment in the setting of mr-guided radiation therapy of prostate cancer on an mr-linac at 1.5 t: A comparison to a standard 3 t mri. Cancers (Basel) 2021;13. https://doi.org/10.3390/cancers13071533.

[14] Nyholm T, Jonsson J, Söderström K, Bergström P, Carlberg A, Frykholm G, et al. Variability in prostate and seminal vesicle delineations defined on magnetic

resonance images, a multi-observer, -center and -sequence study. Radiat Oncol 2013;8. https://doi.org/10.1186/1748-717X-8-126.

[15] Pogson EM, Begg J, Jameson MG, Dempsey C, Latty D, Batumalai V, et al. A phantom assessment of achievable contouring concordance across multiple treatment planning systems. Radiother Oncol 2015;117:438–41. https://doi.org/10.1016/j.radonc.2015.09.022.

[16] Morrow NV, Lawton CA, Qi XS, Li XA. Impact of computed tomography image quality on image-guided radiation therapy based on soft tissue registration. Int J Radiat Oncol Biol Phys 2012;82:e733–8. https://doi.org/10.1016/j.ijrobp.2011.11.043.